Abdominal Radiology (2019) 44:1785–1794
https://doi.org/10.1007/s00261-018-01892-2

HEPATOBILIARY

Prediction of liver remnant regeneration after living donor liver transplantation using preoperative CT texture analysis

Ji-Eun Kim[1] · Jung Hoon Kim[1,2,3] · Sang Joon Park[1] · Seo-Youn Choi[4] · Nam-Joon Yi[5] · Joon Koo Han[1,2,3]

Published online: 5 January 2019

Abstract

Purpose To predict the rate of liver regeneration after living donor liver transplantation (LDLT) using pre-operative computed tomography (CT) texture analysis.

Materials and methods 112 living donors who performed right hepatectomy for LDLT were included retrospectively. We measured the volume of future remnant liver (FLR) on pre-operative CT and the volume of remnant liver (LR) on follow-up CT, taken at a median of 123 days after transplantation. The regeneration index (RI) was calculated using the following equation: $[(V_{LR} - V_{FLR})/V_{FLR}] \times 100$. Computerized texture analysis of the semi-automatically segmented FLR was performed. We used a stepwise, multivariable linear regression to assess associations of clinical features and texture parameters in relation to RI and to make the best-fit predictive model.

Results The mean RI was $110.7 \pm 37.8\%$, highly variable ranging from 22.4% to 247.0%. Among texture parameters, volume of FLR, standard deviation, variance, and gray level co-occurrence matrices (GLCM) contrast were found to have significant correlations between RI. In multivariable analysis, smaller volume of FLR (ß −0.17, 95% CI −0.22 to −0.13) and lower GLCM contrast (ß −1.87, 95% CI −3.64 to −0.10) were associated with higher RI. The regression equation predicting RI was following: RI = 203.82 + 10.42 × pre-operative serum total bilirubin (mg/dL) − 0.17 × V_{FLR} (cm^3) − 1.87 × GLCM contrast (× 100).

Conclusion Volume of FLR and GLCM contrast were independent predictors of RI, showing significant negative correlations. Pre-operative CT with texture analysis can be useful for predicting the rate of liver regeneration in living donor of liver transplantation.

Keywords Liver · Liver transplantation · Tissue Donor · Regeneration · Tomography

Abbreviations

LDLT	Living donor liver transplantation
CT	Computed tomography
ROIs	Regions of interest
FLR	Future liver remnant
SD	Standard deviation
GLCM	Gray-Level Co-occurrence Matrix
ASM	Angular second moment
IDM	GLCM inverse difference moment
LR	Liver remnant
AIC	Akaike information criteria
VIF	Variance inflation factor
CIs	Confidence intervals

✉ Jung Hoon Kim
jhkim2008@gmail.com

1 Department of Radiology, Seoul National University Hospital, 101 Daehak-ro, Jongno-gu, Seoul 03080, Republic of Korea

2 Department of Radiology, Seoul National University College of Medicine, Seoul, Republic of Korea

3 Institute of Radiation Medicine, Seoul National University Medical Research Center, Seoul, Republic of Korea

4 Department of Radiology, Soonchunhyang University Bucheon Hospital, Bucheon-Si, Gyeonggi-Do, South Korea

5 Department of Surgery, Seoul National University Hospital, Seoul, Republic of Korea

Introduction

Demand for liver transplantation has been continuously growing for treatment of several liver diseases but the deceased donor pool is limited. Hence, living donor liver transplantation (LDLT) has been playing an important role in order to solve this problem of donor shortage. However, the

challenge associated with LDLT is that the procedure is with low but definite risk of the donor. Currently, right lobe grafts are most commonly used in LDLT, which causes concern about donor safety because more than half of the liver is resected in the donor [1–4]. Donor safety as well as recipient survival should be considered when planning LDLT. An optimal regeneration of remnant liver in donor is an integral part of successful LDLT. The greatest interest of both the transplant surgeon and donor is whether the donor's remnant liver will be regenerated as in the previous healthy state without complications [5, 6].

Imaging modalities are very helpful in the evaluation of liver regeneration as they can quantify the increase in liver volume objectively. In particular, multidetector computed tomography (CT) has been proven to be an accurate method for the assessment of liver volume and is widely used for the follow-up evaluation after transplantation [7–9]. Therefore, in current practice, volumetric CT is used as the main imaging modality for evaluating donor candidates [7, 10–12].

Quantitative texture analysis is an objective approach for evaluating tissue gray-level patterns that are not otherwise perceptible to human eyes, and is emerging as a useful technique for assessing tissue heterogeneity [13]. This technique relies on objective, computer-assisted measurements and is, therefore, free from subjective biases based on visual interpretation of radiologists [14]. Because of its more sensitive perception of lesion heterogeneity than human eyes, texture analysis is now widely used in variable fields of imaging [13, 15–17].

There have been efforts to predict the ability of liver regeneration with volumetric CT analysis [18]. However, to date, there have been no studies focusing on the relationship between results of CT texture analysis and rate of liver regeneration. The purpose of this study was to evaluate the role of CT texture analysis for predicting the rate of liver regeneration after right hepatectomy in living donors after LDLT.

Materials and methods

Patients

This retrospective study was approved by our institutional review board, and the requirement for obtaining written, informed consent was waived. We analyzed the medical records of 214 living donors for LDLT between January 2010 and December 2011. Details of patient selection for this study are described in Fig. 1. Consequently, a total of 112 donors who underwent right hepatectomy were included for analysis (M:F = 79:33; mean age, 31 years). All of the donors were without a history of chronic liver diseases and showed normal results of liver function tests. Follow-up CT scans were performed 4 months after transplantation according to the protocol of our institution.

CT techniques

All pre-operative CT examinations were performed using the same CT scanner (Somatom Definition, Siemens Healthcare, Forchheim, Germany). For contrast enhancement, 1.5 mL/kg of a 350 mg/mL Iobitridol (Xenetix 350, Guerbet) or Iohexol (Bonorex 350, CMS) was injected at a rate of 3 mL/s using an automatic power injector (Envision CT,

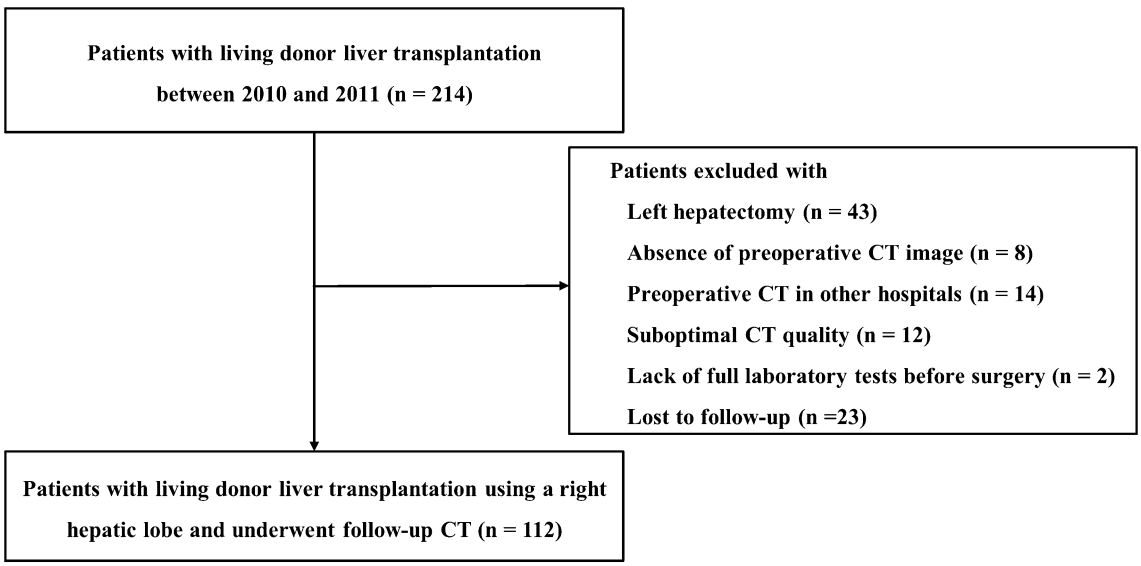

Fig. 1 Illustrated flow charts of patient enrollment

Medrad, Pittsburgh, PA, USA). Arterial phase scanning was performed 19 s after obtaining 100 HU attenuation of the descending aorta measured using a bolus tracking method. For the portal venous phase scan, images were obtained 33 s after the acquisition of the arterial phase scan. After the acquisition of the portal venous phase scan, an additional delayed phase scanning was performed 3 min following contrast agent administration. All of these four-phase scan images were obtained in a dual-energy mode using the following parameters: collimation, 14 × 1.2 mm; rotation time, 0.5 s; and pitch, 0.85. Tube voltages were set at 80 and 140 kVp. The 4D dose modulation protocol provided by the manufacturer (Care Dose 4D, Siemens Medical Solutions) was used to adjust the tube current in a real-time manner in order to maintain image noise at the optimal level. The reference tube current time product was set at 80 mAs for a 140 kVp tube and at 340 mAs for an 80 kVp tube so as to match the noise level to the greatest possible extent. These reference tube currents were chosen so that the acquired images would be approximately dose-matched compared to those acquired using single source CT at 120 kVp. All of the images were reconstructed with an iterative reconstruction in image space (IRIS; Siemens Healthcare) using the I30f kernel (3-mm thickness at 2-mm intervals).

Volumetric CT and computerized texture analysis

For liver segmentation with automated quantification of the texture features, we applied the personal computer–based, in-house software program (MISSTA; Medical Imaging Solution for Segmentation and Texture Analysis) using dedicated C++ language (Microsoft Foundation Classes, Microsoft, Redmond, WA, USA). The portal venous phase images of the pre-operative CT scan acquired at 140 kVp were selected for texture analysis.

First, the entire liver was semi-automatically segmented by an attending radiologist (OOO, with 4 years of abdominal CT clinical experience). Among a set of CT section images of each patient, a few slice images were selected and regions of interest (ROIs) were manually drawn by tracing the liver contour with a computer mouse. After the ROIs were drawn, our software program automatically segmented the whole liver. Liver boundaries were defined as perihepatic fat tissue between the liver and adjacent organs. At the same time, the vena cava, hepatic vein, portal vein, and gallbladder were excluded from the ROIs in order to include only hepatic parenchyma. Then the same attending radiologist visually confirmed the virtually constructed images and manually adjusted them as required in order to ensure the accuracy. Finally, our software program automatically segmented the whole liver, calculated the pixels included within the traced contours on each section, and provided the cross-sectional area of the section on a section-by-section basis. It also provided the three-dimensional virtual image of the liver. Automated segmentation was performed with interactive graph-cut technique which operates base on statistical shape model using global optimization of a cost function including intensity map [19]. (Figure 2). After the entire liver was virtually constructed, the same radiologist drew a plane by referencing the post-operative CT scan to determine the boundary dividing the left and right liver [20]. Subsequently, the software program calculated the volume and texture features of the left liver, which would be the future liver remnant (FLR) after right hepatectomy. In this software program, we used total variation minimization techniques as a filtration step [21]. Computerized texture analysis was performed, automatically extracting 13 quantitative parameters including mean attenuation, standard deviation (SD), variance, skewness, kurtosis, entropy, homogeneity, surface area, sphericity, Gray-Level Co-occurrence Matrix (GLCM) angular second moment (ASM), GLCM inverse difference moment (IDM), GLCM contrast, and GCLM entropy. We also did the same procedure as described above using the four-month follow-up CT images and obtained data of the liver remnant (LR), which represent the result of liver regeneration over four months. Therefore, we could obtain volume data for both the FLR and LR (Fig. 3). With these obtained volumetric parameters, we calculated the regeneration index (RI) as follows: $\left[\left(V_{LR} - V_{FLR}\right)/V_{FLR}\right] \times 100\,(\%)$ [22].

Statistical analysis

We intended to determine the predictive factors of RI calculated as described above. First, we compared the demographic characteristics and texture features according to the RI level, using the cut-off level of 100%. Then, correlations between RI and several variables, including not only texture features but also demographic and laboratory characteristics, were evaluated using a linear regression analysis. A stepwise multivariable regression analysis was then performed in order to determine the most appropriate predictors of RI. Variables with *P* values less than 0.1 in univariable analysis were included in multivariable analysis. For selection of the best-fit model, we used the Akaike information criteria (AIC) which is a measure of a statistical model's goodness of fit [23]. The variance inflation factor (VIF) was used to examine the multicollinearity between variables. A maximum VIF of less than 4 was used as a cut-off for indicating independence of the variables. Results of regression analysis were described as regression coefficient (ß) of the independent variable with 95% confidence intervals (CIs). *P* values less than 0.05 were considered statistically significant in a two-tailed test. Statistical analysis was conducted using SPSS software version 22.0 (IBM Corp., Armonk, NY, USA).

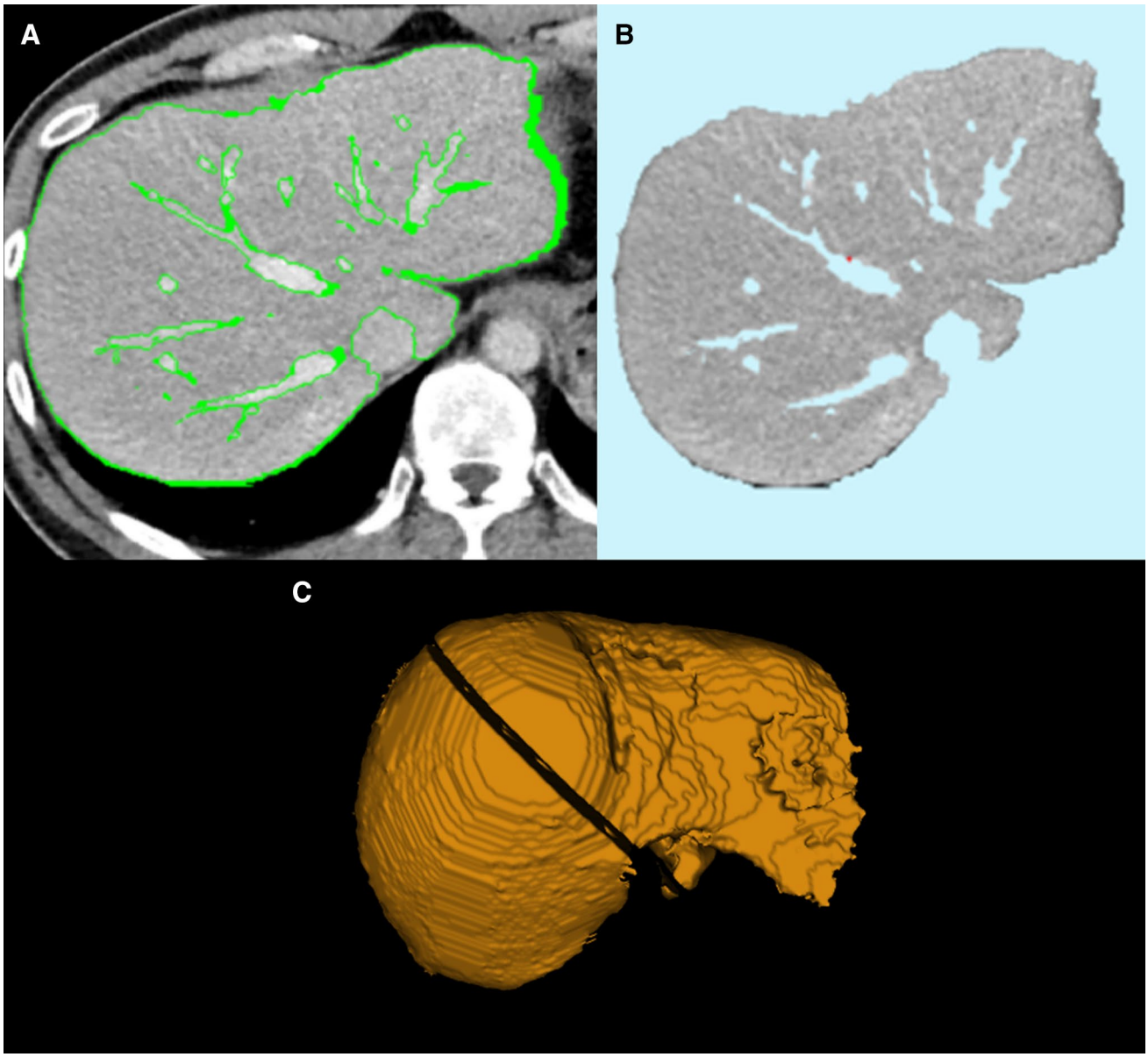

Fig. 2 Liver segmentation using in-house software program. **a** Semi-automatically segmented liver. **b** Extracted liver parenchyma. **c** A surgical resection plane by referencing post-operative computed tomography scan to determine the boundary dividing left and right liver

Results

Demographic characteristics and laboratory findings of the donors

The demographic characteristics and laboratory findings of the donors are summarized in Table 1. The mean graft weight and graft-to-recipient weight ratio were 728.1 ± 150.9 g and 1.13 ± 0.28%, respectively. There were no operation-related mortalities and post-hepatectomy liver failures, and the mean estimated blood loss during surgery was 293 mL. However, biliary stricture occurred in one patient, thus requiring an endoscopic biliary drainage procedure. Another patient developed post-operative pulmonary edema and acute kidney injury, both of which eventually improved without long-term sequelae.

The mean volume of the FLR was 520.24 ± 124.40 cm^3. Follow-up CT scans were performed at a median of 123 (interquartile 120–130 days) days after surgery. On follow-up CT, the mean volume of the LR was 1068.04 ± 198.21 cm^3. The mean RI was 110.7 ± 37.8%, highly variable ranging from 22.4% to 247.0%. Figure 4 shows the distribution of the RI. We classified it into the higher RI group and the lower RI group according to an

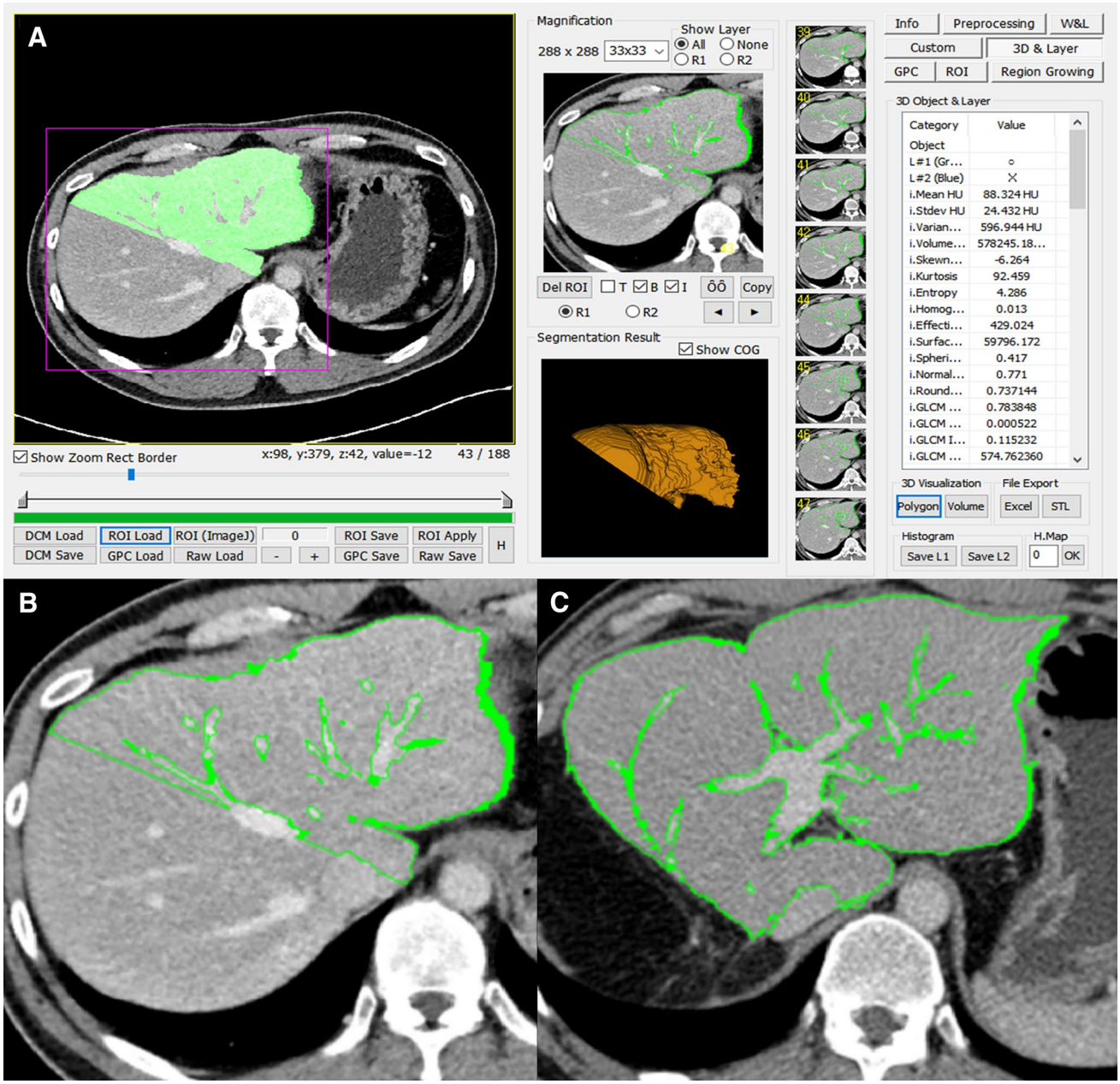

Fig. 3 Computerized texture analysis using in-house software program. **a** The in-house software program calculated the volume data and texture data of the left liver. **b** The volume and texture data obtained from the future liver remnant after right hepatectomy. **c** In 4-month follow-up computed tomography images, we obtained volume and texture data of the regenerated liver

RI level of 100%. Among 112 donors, 63 (56.2%) had an RI of 100% or more (higher RI group) and 49 (43.8%) donors had an RI less than 100% (lower RI group). Among the baseline characteristics, there were no significant differences between the higher RI group and the lower RI group. The LR volume also did not differ between two groups ($P = 0.254$). However, the FLR volume was significantly lower in the higher RI group. The mean FLR volume was 464.28 ± 89.62 cm^3 in the higher RI group and 592.20 ± 126.56 cm^3 in the lower RI group ($P < 0.001$).

Important texture features and clinical findings for predicting liver regeneration

The results of the texture analysis are summarized in Table 2. The higher RI group had a significantly lower surface area than lower RI group ($P < 0.001$). The GLCM contrast value was also lower in the higher RI group without statistically significance ($P = 0.080$). Table 3 summarizes the results of regression analysis for predicting the rate of liver regeneration. The serum total bilirubin level showed

Table 1 Summary of demographic characteristics and laboratory findings of the donors

Characteristics	Total ($N=112$)	Lower RI ($N=49$)	Higher RI ($N=63$)	P value
Age (year)	31 ± 10	30 ± 11	31 ± 10	0.566
Male sex (%)	79 (70.5%)	33 (67.4%)	46 (73.0%)	0.514
Body weight (kg)	66.1 ± 10.9	66.5 ± 11.2	65.8 ± 10.7	0.752
Body mass index (kg/m$^{2)}$	23.0 ± 3.0	23.0 ± 3.1	23.0 ± 3.1	0.888
Pre-operative plasma serum levels				
Hemoglobin (g/dL)	14.9 ± 1.6	14.8 ± 1.7	15.1 ± 1.5	0.366
White blood cell ($\times 10^3$/μL)	6.02 ± 1.34	6.09 ± 1.41	5.96 ± 1.30	0.631
Platelet ($\times 10^3$/μL)	239.4 ± 52.1	244.3 ± 47.5	235.5 ± 55.6	0.377
Prothrombin time (INR)	1.01 ± 0.06	1.00 ± 0.05	1.02 ± 0.06	0.052
Total bilirubin (mg/dL)	0.9 ± 0.5	0.9 ± 0.4	1.0 ± 0.5	0.272
Direct bilirubin (mg/dL)	0.2 ± 0.1	0.2 ± 0.1	0.2 ± 0.1	0.814
AST (IU/L)	19.8 ± 5.4	20.1 ± 5.2	19.6 ± 5.6	0.654
ALT (IU/L)	20.8 ± 11.6	21.4 ± 10.6	20.4 ± 12.5	0.634
GGT (IU/L)	26.2 ± 17.3	27.2 ± 18.9	25.4 ± 16.0	0.596
Albumin (g/dL)	4.6 ± 0.3	4.5 ± 0.3	4.6 ± 0.3	0.208
Liver volume (cm^3)				
Future remnant liver volume	520.24 ± 124.40	592.20 ± 126.56	464.28 ± 89.62	< 0.001
Remnant liver volume	1068.04 ± 198.21	1043.70 ± 201.52	1086.96 ± 195.09	0.254
Regeneration index (%)	110.7 ± 37.8	77.9 ± 17.0	136.2 ± 28.7	< 0.001

Data were presented mean ± standard deviation for continuous variables and n (%) for categorical variables

RI regeneration index, *INR* international normalized ratio, *AST* aspartate transaminase, *ALT* alanine transaminase, *GGT* gamma glutamyl transpeptidase

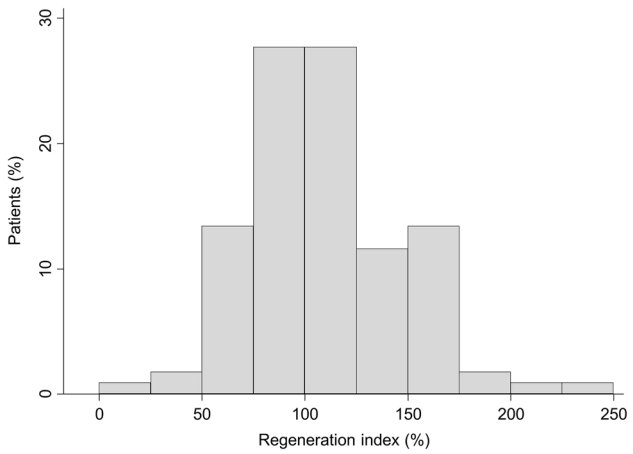

Fig. 4 The distribution of regeneration index

marginal association with RI (ß coefficient 14.32, 95% CI − 1.17–29.81, $P=0.070$). The volume of FLR (ß coefficient − 0.18, 95% CI − 0.23 to − 0.14, $P<0.001$) and the surface area (ß coefficient − 0.15, 95% CI − 0.21 to − 0.10, $P<0.001$) had significant negative linear association with RI. When the resected volume was larger and the FLR was smaller, the RI was higher after four months of regeneration. Among other texture features, SD (ß coefficient − 1.14, 95% CI − 2.17 to − 0.11, $P=0.013$), variance (ß coefficient − 0.02, 95% CI − 0.03–0.00, $P=0.038$), and GLCM contrast (ß coefficient − 2.89, 95% CI − 5.08 to − 0.71, $P=0.010$) showed statistically significant association with the RI. Patient age, sex, and laboratory findings other than bilirubin level did not show statistically significant association with the RI.

Prediction model of regeneration index using multivariable regression

For the best-fit predictive model of the RI, we performed a stepwise multivariable regression and found that the volume and surface area of FLR and the GLCM contrast showed significant effects on the RI (Table 5 Model 2). However, both the volume and surface area of FLR showed a VIF higher than 4, which suggests the possibility of significant collinearity. Therefore, we subsequently adjusted the model in order to determine the best-fit model (Table 5 Models 3 and 4). Finally, the pre-operative serum total bilirubin level, the volume of FLR, and the GLCM contrast were found to be the best independent predictors of RI (Table 4). A smaller volume of FLR (ß coefficient − 0.17, 95% CI − 0.22 to − 0.13, and $P<0.001$) and lower GLCM contrast (ß coefficient − 1.87, 95% CI − 3.64 to − 0.10, and $P=0.038$) were associated with higher RI. The association of the FLR volume and the GLCM contrast in relation to the RI are demonstrated in Figs. 5 and 6. A slightly elevated pre-operative total bilirubin level, even though it was within the normal range, was associated with

Table 2 Comparison of texture features between lower RI and higher RI groups

Texture features	Total ($N=112$)	Lower RI ($N=49$)	Higher RI ($N=63$)	P value
Mean attenuation of pixels (HU)	102.5 ± 8.6	102.4 ± 9.9	102.6 ± 7.5	0.914
SD of pixel attenuation (HU)	31.1 ± 6.8	32.2 ± 7.4	30.3 ± 6.2	0.147
Variance (HU)	1015.2 ± 455.9	1089.9 ± 506.5	957.1 ± 406.9	0.127
Skewness	− 6.7 ± 2.1	− 6.9 ± 2.1	− 6.6 ± 2.1	0.495
Kurtosis	92.5 ± 38.9	94.3 ± 40.4	91.1 ± 38.0	0.671
Entropy	4.4 ± 0.1	4.4 ± 0.2	4.4 ± 0.1	0.625
Homogeneity ($\times 10^{-3}$)	11.1 ± 1.3	11.2 ± 1.6	11.1 ± 1.1	0.665
Surface area (cm^2)	513.6 ± 111.0	566.1 ± 118.8	472.9 ± 85.4	< 0.001
Sphericity	0.4 ± 0.0	0.4 ± 0.0	0.4 ± 0.0	0.160
GLCM ASM ($\times 10^{-3}$)	4.0 ± 2.2	3.9 ± 2.6	4.0 ± 1.8	0.820
GLCM IDM	0.4 ± 0.1	0.4 ± 0.1	0.4 ± 0.1	0.258
GLCM contrast ($\times 10^2$)	6.6 ± 3.2	7.1 ± 3.4	6.1 ± 2.9	0.080
GLCM entropy	2.9 ± 0.3	3.0 ± 0.4	2.9 ± 0.2	0.158

Data were presented as mean ± standard deviation. The donors were divided into two groups according to the RI level, using the cut-off level of 100%

RI regeneration index, *SD* standard deviation, *GLCM* gray-level co-occurrence matrix, *ASM* angular second moment, *IDM* inverse difference moment

higher RI without statistically significance. Consequently, the regression equation predicting the RI was designed as the following: expected RI = 203.82 + 10.42 × pre-operative serum total bilirubin (mg/dL) − 0.17 × V_{FLR} (cm^3) − 1.87 × GLCM contrast (× 100).

Discussion

With increasing numbers of LDLT, there is an increasing concern regarding the donor safety. Donor safety must be the first priority during the entire process of LDLT. It is well-known that the graft-to-recipient body weight ratio should be at least 0.8% in order to prevent the small-for-size syndrome in the recipient. On the other hand, a sufficiently large liver volume should remain in the donors so as to meet the metabolic demand until the remnant regenerates to a sufficient size. In this regard, there have been attempts to use left lobe rather than right lobe for transplantation, which would reduce the donor risk [3, 24]. However, most of the transplantation centers are using right lobe grafts. Therefore, it would be very helpful if we can predict the regeneration potency in planning stage for preventing unexpected post-hepatectomy liver failure in donor.

In our study, the mean RI was 110.7 ± 37.8% with highly variable ranging from 22.4 to 247.0%. In multivariable regression, the volume of FLR and GLCM contrast were shown to be the independent variables for predicting the RI using pre-operative CT. The lower GLCM contrast (ß coefficient = − 1.87, 95% CI − 3.64 to − 0.10, $P = 0.038$) were associated with higher RI. The texture features from GLCM analyses represent the spatial distribution of gray-levels, which indicates how often a pixel of one gray-level is found with a certain relationship to another gray-level pixel [25, 26]. As GLCM contrast is a measurement of local variation in GLCM matrix, a significant change in the gray-level of an adjacent pixel is more likely to contribute to high GLCM contrast than a gradual change in the gray-level over a large area. In our results, higher GLCM contrast of the FLR were negatively associated with regeneration capacity. Considering the previous findings showing that the potential of liver regeneration decreases with repeated chemotherapy or in the presence of moderate-to-severe hepatic steatosis, microscopic heterogeneity of liver parenchyma not detected by conventional imaging may have a substantial influence on the potential of liver regeneration [27–29]. This may be the reason why different liver donors show varying abilities in restoring their original liver volume after surgery, even though they are carefully selected healthy donors. Therefore, pre-operative texture analysis and assessment of tissue heterogeneity may provide additional information for predicting liver regeneration [30].

The volume of FLR (ß coefficient = − 0.17, 95% CI − 0.22 to − 0.13, $P < 0.001$) was also shown to be related to higher RI and this finding has been consistently shown in previous studies [1, 31–33]. Although resection of larger volume of liver can result in more effective hepatic proliferation, it is important not to resect too large a volume of liver to reduce the risk of liver failure. Therefore, it is imperative to evaluate the volume of remnant liver and to predict regeneration potency of liver in planning stage. We suggested regression equation predicting RI of liver using pre-operative CT images. We expect that pre-operative texture analysis may provide additional help for successfully predicting liver regeneration.

Table 3 Summary of important clinical and texture features for hepatic regeneration

Variables	Unstandardized regression coefficient (95% CI)	*P* value
Age (year)	0.31 (−0.40–1.03)	0.387
Male sex	4.20 (−11.39–19.80)	0.594
Body mass index (kg/m^2)	−0.52 (−2.87–1.84)	0.664
Hemoglobin (g/dL)	1.43 (−3.01–5.88)	0.527
White blood cell (×10^3/μL)	−2.30 (−7.26–2.67)	0.361
Platelet (×10^3/μL)	0.01 (−0.01–0.03)	0.171
Prothrombin time (INR)	111.48 (−6.21–229.17)	0.063
Total bilirubin (mg/dL)	14.32 (−1.17–29.81)	0.070
AST (IU/L)	−1.13 (−2.42–0.17)	0.089
ALT (IU/L)	−0.38 (−0.99–0.23)	0.216
Albumin (g/dL)	−6.27 (−30.43–17.88)	0.608
V_{FLR} (cm^3)	−0.18 (−0.23 to −0.14)	<0.001
Mean (HU)	0.15 (−0.68–0.99)	0.714
SD (HU)	−1.14 (−2.17 to −0.11)	0.031
Variance (HU)	−0.02 (−0.03–0.00)	0.038
Skewness	2.69 (−0.69–6.06)	0.118
Kurtosis	−0.08 (−0.27–0.10)	0.360
Entropy	−7.21 (−54.97–40.55)	0.765
Homogeneity (×10^{-3})	−1.53 (−6.87–3.81)	0.572
Surface area (cm^2)	−0.15 (−0.21 to −0.10)	<0.001
Sphericity	67.18 (−116.77–251.12)	0.471
GLCM ASM (×10^{-3})	−0.76 (−4.06–2.54)	0.650
GLCM IDM	13.09 (−45.2–71.39)	0.657
GLCM contrast (×10^2)	−2.89 (−5.08 to −0.71)	0.010
GLCM entropy	−8.93 (−30.75–12.89)	0.419

The regression coefficients were calculated using a univariable linear regression of regeneration index on each variable

CI confidence interval, *INR* international normalized ratio, *AST* aspartate transaminase, *ALT* alanine transaminase, V_{FLR} volume of future remnant liver, *SD* standard deviation, *GLCM* gray-level co-occurrence matrix, *ASM* angular second moment, *IDM* inverse difference moment

Table 4 Important clinical and texture features for prediction of hepatic regeneration

Variables	Unstandardized regression coefficient (95% CI)	*P* value	Variance inflation factor
Total bilirubin (mg/dL)	10.42 (−1.85–22.69)	0.095	1.01
V_{FLR} (cm^3)	−0.17 (−0.22 to −0.13)	<0.001	1.02
GLCM contrast (×10^2)	−1.87 (−3.64 to −0.10)	0.038	1.02

A stepwise multivariable linear regression was performed and the best-fit model was selected using the Akaike information criteria

CI confidence interval, V_{FLR} volume of future remnant liver, *GLCM* gray-level co-occurrence matrix

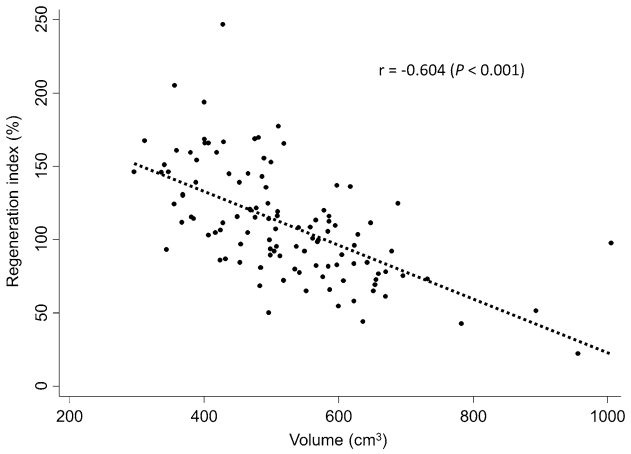

Fig. 5 The correlation of the volume of future liver remnant (FLR) and regeneration index (RI). Smaller volume of FLR were associated with higher RI

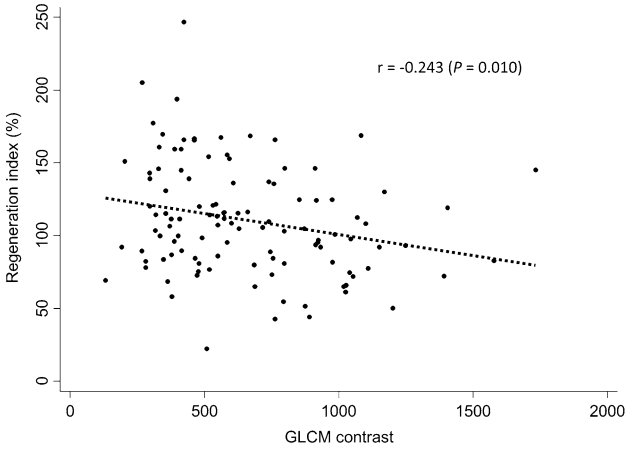

Fig. 6 The correlation of the gray level co-occurrence matrix (GLCM) contrast and regeneration index (RI). Lower GLCM contrast were associated with higher RI

An interesting result of our study is that the subclinical elevation of pre-operative serum bilirubin had a marginal negative effect on liver regeneration. In previous studies, an obvious relationship has been observed between the pre-operative serum bilirubin level and the frequency of complications after liver resection [34, 35]. In addition, pre-operative biliary drainage has also been shown to influence the amount of liver regeneration occurring after surgery [36, 37]. These findings suggest that the bile itself may contain some important factors involved in hepatocyte regeneration. However, although frank cholestasis due to biliary obstruction has been shown to limit the liver regeneration, there are no conclusive data regarding whether the subclinical level of cholestasis also affects the liver regeneration and more studies are, therefore, needed.

There are several limitations in our study. First, as our study was a retrospective study, there is the possibility of selection bias. Second, the exact histopathology related to increased tissue heterogeneity, detected by texture analysis, was not identified due to the lack of a histopathologic examination. Further studies in a large number of patients undergoing liver resection will be needed in order to identify the histopathologic significance of the abnormal findings shown in texture analysis. Third, our study was focused on regeneration of the liver in only donor, not recipient. The environment for regeneration is quite different between the healthy donor and the recipient recovering from hepatic failure. The relationship between the tissue texture of a transplant liver graft and its ability to regenerate in the recipient should also be elucidated in future studies. Despite these limitations, our study showed that texture analysis could be a promising tool in predicting post-operative liver regeneration in individual living liver donors. A comprehensive, prospective study is needed in order to confirm our results and to establish the role of texture analysis in LDLT.

In conclusion, the increased hepatic parenchymal heterogeneity shown in CT texture analysis was shown to have a negative effect on liver regeneration after right hepatectomy in a living donor undergoing LDLT. In addition, the volume of FLR had an influence on the rate of regeneration. Our study provides preliminary evidence of the relationship between the texture features and the potency of liver regeneration. Therefore, CT with texture analysis could be useful for predicting the potential of liver regeneration in LDLT, thus leading to more successful transplantation.

Acknowledgements We would like to thank Bonnie Hami, MA (USA) and Seunghyun Kim for her editorial assistance in the preparation of this manuscript.

Compliance with ethical standards

Conflict of interest All authors confirm that no disclosure of potential conflicts of interest.

Ethical approval This retrospective study was approved by our institutional review board, and the requirement to obtain written, informed consent was waived.

Appendix

See Table 5.

Table 5 Models for predicting regeneration index

Models and variables	Unstandardized regression coefficient (95% CI)	*P* value	Variance inflation factor
Model 1			
Prothrombin time (INR)	− 17.34 (− 115.03–80.35)	0.726	1.17
Total bilirubin (mg/dL)	10.82 (− 1.72–23.37)	0.090	1.10
AST (IU/L)	− 0.47(− 1.57–0.63)	0.400	1.20
V_{FLR} (cm^3)	− 0.32 (− 0.41 to − 0.22)	< 0.001	4.70
SD (HU)	0.88 (− 5.20–6.95)	0.776	57.95
Variance (HU)	− 0.01 (− 0.10–0.07)	0.818	55.84
Surface area (cm^2)	0.19 (0.08–0.30)	0.001	5.17
GLCM contrast ($\times 10^2$)	− 3.41 (− 6.83–0.01)	0.050	3.97
Model 2			
Total bilirubin (mg/dL)	11.24 (− 0.50–22.98)	0.060	1.01
V_{FLR} (cm^3)	− 0.31 (− 0.40 to − 0.22)	< 0.001	4.68
Surface area (cm^2)	0.18 (0.07–0.29)	0.001	4.98
GLCM contrast ($\times 10^2$)	− 2.88 (− 4.67 to − 1.08)	0.002	1.15
Model 3			
Total bilirubin (mg/dL)	10.42 (− 1.85–22.69)	0.095	1.01
V_{FLR} (cm^3)	− 0.17 (− 0.22 to − 0.13)	< 0.001	1.02
GLCM contrast ($\times 10^2$)	− 1.87 (− 3.64 to − 0.10)	0.038	1.02
Model 4			
Total bilirubin (mg/dL)	11.00 (− 2.92–24.92)	0.120	1.01
Surface area (cm^2)	− 0.14 (− 0.20 to − 0.08)	< 0.001	1.09
GLCM contrast ($\times 10^2$)	− 1.47 (− 3.54–0.59)	0.161	1.08

CI confidence interval, *INR* international normalized ratio, *AST* aspartate transaminase, V_{FLR} volume of future remnant liver, *SD* standard deviation, *GLCM* gray-level co-occurrence matrix

References

1. Haga J, Shimazu M, Wakabayashi G, et al. (2008) Liver regeneration in donors and adult recipients after living donor liver transplantation. Liver Transpl 14:1718–1724
2. Taner CB, Dayangac M, Akin B, et al. (2008) Donor safety and remnant liver volume in living donor liver transplantation. Liver Transpl 14:1174–1179
3. Kim PT, Testa G (2016) Living donor liver transplantation in the USA. Hepatobiliary Surg Nutr 5:133–140
4. Broelsch CE, Burdelski M, Rogiers X, et al. (1994) Living donor for liver transplantation. Hepatology 20:49S–55S
5. Lee SY, Ko GY, Gwon DI, et al. (2004) Living donor liver transplantation: complications in donors and interventional management. Radiology 230:443–449
6. Hashikura Y, Ichida T, Umeshita K, et al. (2009) Donor complications associated with living donor liver transplantation in Japan. Transplantation 88:110–114
7. Kamel IR, Kruskal JB, Warmbrand G, et al. (2001) Accuracy of volumetric measurements after virtual right hepatectomy in potential donors undergoing living adult liver transplantation. AJR Am J Roentgenol 176:483–487
8. Emiroglu R, Coskun M, Yilmaz U, et al. (2006) Safety of multidetector computed tomography in calculating liver volume for living-donor liver transplantation. Transplant Proc 38:3576–3578
9. Joyeux H, Berticelli J, Chemouny S, Masson B, Borianne P (2003) Semi-automatic measurements of hepatic lobes. Application to study of liver volumes. Analysis of 50 computed tomography of normal liver. Ann Chir 128:251–255
10. Leelaudomlipi S, Sugawara Y, Kaneko J, et al. (2002) Volumetric analysis of liver segments in 155 living donors. Liver Transpl 8:612–614
11. Kim SJ, Kim DG, Chung ES, et al. (2006) Adult living donor liver transplantation using the right lobe. Transplant Proc 38:2117–2120
12. Hiroshige S, Shimada M, Harada N, et al. (2003) Accurate preoperative estimation of liver-graft volumetry using three-dimensional computed tomography. Transplantation 75:1561–1564
13. Kassner A, Thornhill RE (2010) Texture analysis: a review of neurologic MR imaging applications. AJNR Am J Neuroradiol 31:809–816
14. Tourassi GD (1999) Journey toward computer-aided diagnosis: role of image texture analysis. Radiology 213:317–320
15. Bayanati H, Thornhill RE, Souza CA, et al. (2015) Quantitative CT texture and shape analysis: can it differentiate benign and malignant mediastinal lymph nodes in patients with primary lung cancer? European Radiology 25:480–487
16. Ravanelli M, Farina D, Morassi M, et al. (2013) Texture analysis of advanced non-small cell lung cancer (NSCLC) on contrast-enhanced computed tomography: prediction of the response to the first-line chemotherapy. European Radiology 23:3450–3455
17. Ganeshan B, Abaleke S, Young RCD, Chatwin CR, Miles KA (2010) Texture analysis of non-small cell lung cancer on unenhanced computed tomography: initial evidence for a relationship with tumour glucose metabolism and stage. Cancer Imaging 10:137–143
18. Olthoff KM, Emond JC, Shearon TH, et al. (2015) Liver regeneration after living donor transplantation: adult-to-adult living donor liver transplantation cohort study. Liver Transpl 21:79–88
19. Boykov YY, Jolly M-P (2001) Interactive graph cuts for optimal boundary & region segmentation of objects in ND imagesComputer Vision, 2001 ICCV 2001 Proceedings Eighth IEEE International Conference on. IEEE, pp 105-112
20. Ger R (1989) Surgical anatomy of the liver. Surg Clin North Am 69:179–192
21. Chambolle A (2004) An algorithm for total variation minimization and applications. Journal of Mathematical imaging and vision 20:89–97
22. Zappa M, Dondero F, Sibert A, et al. (2009) Liver regeneration at day 7 after right hepatectomy: global and segmental volumetric analysis by using CT. Radiology 252:426–432
23. Sakamoto T, Ezure T, Lunz J, et al. (2000) Concanavalin A simultaneously primes liver hematopoietic and epithelial progenitor cells for parallel expansion during liver regeneration after partial hepatectomy in mice. Hepatology 32:256–267
24. Botha JF, Langnas AN, Campos BD, et al. (2010) Left lobe adult-to-adult living donor liver transplantation: small grafts and hemiportocaval shunts in the prevention of small-for-size syndrome. Liver Transpl 16:649–657
25. Davnall F, Yip CS, Ljungqvist G, et al. (2012) Assessment of tumor heterogeneity: an emerging imaging tool for clinical practice? Insights Imaging 3:573–589
26. Ganeshan B, Miles KA (2013) Quantifying tumour heterogeneity with CT. Cancer Imaging 13:140–149
27. Ju MK, Choi GH, Park JS, et al. (2012) Difference of regeneration potential between healthy and diseased liver. Transplant Proc 44:338–340
28. Kele PG, van der Jagt EJ, Gouw AS, et al. (2013) The impact of hepatic steatosis on liver regeneration after partial hepatectomy. Liver Int 33:469–475
29. Dello SA, Kele PG, Porte RJ, et al. (2014) Influence of preoperative chemotherapy on CT volumetric liver regeneration following right hemihepatectomy. World J Surg 38:497–504
30. Shimada M, Matsumata T, Maeda T, et al. (1994) Hepatic regeneration following right lobectomy: estimation of regenerative capacity. Surg Today 24:44–48
31. Kwon KH, Kim YW, Kim SI, et al. (2003) Postoperative liver regeneration and complication in live liver donor after partial hepatectomy for living donor liver transplantation. Yonsei Med J 44:1069–1077
32. Paluszkiewicz R, Zieniewicz K, Kalinowski P, et al. (2009) Liver regeneration in 120 consecutive living-related liver donors. Transplant Proc 41:2981–2984
33. Gaglio PJ, Liu H, Dash S, et al. (2002) Liver regeneration investigated in a non-human primate model (Macaca mulatta). J Hepatol 37:625–632
34. Greig JD, Krukowski ZH, Matheson NA (1988) Surgical morbidity and mortality in one hundred and twenty-nine patients with obstructive jaundice. Br J Surg 75:216–219
35. Scheingraber S, Bauer M, Bauer I, et al. (2009) Inhibition of hemoxygenase-1 improves survival after liver resection in jaundiced rats. Eur Surg Res 42:157–167
36. Cherqui D, Benoist S, Malassagne B, et al. (2000) Major liver resection for carcinoma in jaundiced patients without preoperative biliary drainage. Arch Surg 135:302–308
37. Das BC, Isaji S, Kawarada Y (2001) Analysis of 100 consecutive hepatectomies: risk factors in patients with liver cirrhosis or obstructive jaundice. World J Surg 25:266-272; discussion 272-263